Interplanetary magnetic field control of the entry of solar energetic particles into the magnetosphere

R. L. Richard, M. El-Alaoui, M. Ashour-Abdalla,[1] and R. J. Walker[2]
Institute of Geophysics and Planetary Physics, University of California at Los Angeles, Los Angeles, California, USA

Received 2 April 2001; revised 6 February 2002; accepted 18 March 2002; published 15 August 2002.

[1] We have investigated the entry of energetic ions of solar origin into the magnetosphere as a function of the interplanetary magnetic field orientation. We have modeled this entry by following high energy particles (protons and ^{3}He ions) ranging from 0.1 to 50 MeV in electric and magnetic fields from a global magnetohydrodynamic (MHD) model of the magnetosphere and its interaction with the solar wind. For the most part these particles entered the magnetosphere on or near open field lines except for some above 10 MeV that could enter directly by crossing field lines due to their large gyroradii. The MHD simulation was driven by a series of idealized solar wind and interplanetary magnetic field (IMF) conditions. It was found that the flux of particles in the magnetosphere and transport into the inner magnetosphere varied widely according to the IMF orientation for a constant upstream particle source, with the most efficient entry occurring under southward IMF conditions. The flux inside the magnetosphere could approach that in the solar wind implying that SEPs can contribute significantly to the magnetospheric energetic particle population during typical SEP events depending on the state of the magnetosphere. *INDEX TERMS:* 2720 Magnetospheric Physics: Energetic particles, trapped; 2716 Magnetospheric Physics: Energetic particles, precipitating; 2753 Magnetospheric Physics: Numerical modeling; 2784 Magnetospheric Physics: Solar wind/magnetosphere interactions; *KEYWORDS:* Solar energetic particles, magnetosphere, trapping, precipitation

1. Introduction

[2] Solar energetic particles (keV to GeV) are generated at active regions on the Sun and are also accelerated at interplanetary shocks launched by the solar disturbances [*Flückiger*, 1991; *Shea and Smart*, 1995]. These particles can move along interplanetary magnetic field lines to the Earth. Solar energetic particles (SEPs) can reach the ground (solar cosmic ray events), and enhanced proton fluxes can be seen at the top of the atmosphere and in space (solar proton events). It is well established that energetic ions can penetrate the magnetosphere [*Fennell*, 1973]. That particle fluxes at geosynchronous orbit track those in the interplanetary medium [*Kallenrode*, 1998] is evidence of deep penetration of these particles, particularly the ions. It is not presently clear, however, how solar high energy particles (>0.1 MeV) enter, are transported within and exit the magnetosphere [*Gussenhoven et al.*, 1996].

[3] There are two basic types of SEP events, gradual and impulsive [*Kallenrode*, 1998; *Reames*, 1999; *Blanc et al.*, 1999]. Impulsive events last for hours, while gradual events, as the name suggests, are typically longer in duration, lasting for days. While protons, electrons and α particles dominate both kinds of events heavy ions and ^{3}He ions are also present. The two types of events are distinguished by compositional and other differences indicating different acceleration mechanisms. In particular the impulsive events are rich in ^{3}He. The gradual events are correlated with coronal mass ejections that accelerate particles at their accompanying shocks, and impulsive events that evidently originate at solar flares [*Reames*, 1999].

[4] Differential fluxes near 100 keV from a "typical" gradual SEP event in the heliosphere [*Gloeckler et al.*, 1984; *Lin*, 1987] are roughly comparable to those measured in the high energy tail of the proton distribution in the plasma sheet [*Christon et al.*, 1988]. *Reames et al.* [1997] shows a differential flux of a similar magnitude at 100 keV for a gradual event on October 20, 1995 (10^5 protons/(cm^2 sr *S* MeV)). The distribution function for these protons follows a power law distribution ($f \sim E^{-\gamma}$) with $\gamma \cong 2$. *Rodriguez-Pacheco et al.* [1998] fit power laws to ion distributions between 36 and 1600 keV for the most intense energetic particle events of solar cycle 21, mostly gradual events, and found that these power law exponents ranged from 1.25 to 1.94 with a mean of 1.60. *Christon et al.* [1988] found that the high energy part of the plasma sheet spectra followed power laws with exponents around 6.5. Given that the differential fluxes of 100 keV ions in SEPs and in the plasma sheet are comparable, and further if solar energetic particles can penetrate the magnetosphere freely, the much harder (lower power law exponents) SEP spectra

[1] Also at Department of Physics and Astronomy, University of California at Los Angeles, Los Angeles, California, USA.
[2] Also at Department of Earth and Space Science, University of California at Los Angeles, Los Angeles, California, USA.

0148-0227/02/2001JA000099$09.00

imply that these will dominate at higher energies. Note that *Christon et al.* [1988] did not study particles with energies as large as the more energetic SEPs, and this comparison is partly based on extrapolating the plasma sheet energy distributions. These simple estimates suggest that SEPs can be an important component of the magnetospheric particle population during strong SEP events, if they can efficiently enter the magnetosphere. Observations of SEP ions at geosynchronous orbit [*Kallenrode*, 1998] confirm that they can be an important energetic particle source.

[5] Internal acceleration within the magnetosphere during disturbed times can also lead to high-energy injection events. One example of this is the appearance of high energy electrons in the 2 to 6 MeV range associated with periods of high solar wind speed that has been attributed to high inductive electric fields within the magnetosphere [*Baker et al.*, 1998]. *Hudson et al.* [1996] investigated ring current formation by following high energy particles in the equatorial plane in the inner magnetosphere in an MHD model to study how the electrons and protons were accelerated and transported into the ring current. They assumed that the energetic protons were of solar origin and that they had already penetrated the inner magnetosphere. They did not consider how the ions reached this region, which is the topic of this study.

[6] The goal of this study is to understand the entry of SEPs into the magnetosphere and under what conditions they contribute significantly to the magnetospheric particle population. While the most energetic solar particles will not be strongly deflected by magnetospheric magnetic fields, the entry of a large fraction of the incoming energetic particles will be influenced by the magnetospheric configuration, which is controlled in turn by the IMF. We will approach the problem of SEP entry into the magnetosphere by calculating the trajectories of many particle trajectories in MHD field models of the magnetosphere under different IMF conditions. We focus on the transport into the inner magnetosphere that provides the source population for the ring current rather than the evolution of that source population into the ring current population. In the section 2 of this paper we discuss our model and in section 3 we present our results. In section 4 we discuss what we have learned about SEP ion entry.

2. The Model

[7] In this section we describe the model system we used for our calculations. We computed the trajectories of high energy particles subject to the Lorentz force equation including relativistic modifications. Because these high energy particles have large Larmor radii, a guiding center approximation would be inadequate. The electric and magnetic field model in which we determined the trajectories of these particles was obtained from a global magnetohydrodynamic (MHD) simulation of the magnetosphere and its interaction with the solar wind [*Raeder et al.*, 1995]. MHD simulations provide the best three dimensional global models of the entire magnetosphere and its interaction with the solar wind available, as shown by their ability to model spacecraft observations [*Frank et al.*, 1995]. MHD simulations have been used with some success as field models in which to model thermal particle motion in the magnetosphere [*Richard et al.*, 1994, 1997; *Ashour-Abdalla et al.*, 1997]. SEP particles in the solar wind are very tenuous compared to the bulk (low energy) solar wind and they should not perturb the field model significantly, with the possible exception of the ring current region. For this study we primarily launched protons, but we also launched some ^{3}He ions because of their importance as indicators of impulsive solar particle events.

[8] To simplify the interpretation of the results we used idealized solar wind and IMF conditions (Figure 1) to drive the simulation. The y and z components of the IMF were assumed to vary during the simulation (Figure 1) while the IMF x component was held at -5 nT. For the first hour and a half of the simulation, B_z was southward with a magnitude of 5 nT to initialize the simulation. From 1.5 to 3.5 hours B_z was southward with a magnitude of 8 nT. A two hour interval of steady IMF allowed the model magnetosphere to respond to this driving condition. Previous MHD simulations have shown that a timescale of one to two hours is needed for the magnetosphere to reach a new configuration following a change in the IMF [*Ogino et al.*, 1994; *Walker et al.*, 1999]. During this southward IMF interval solar wind, i.e. not connected to the Earth, field lines reconnected with closed field lines on the dayside, while in the magnetotail open field lines reconnected to make solar wind and closed field lines. We varied the IMF linearly in time between 3 hours 30 min and 4 hours until it was dawnward and then held it steady with $B_y = 8$ nT from hours 4 to 6. This led to a magnetospheric configuration with open field lines on the dawn side flank of the magnetosphere. From hour 6 to 6 hours 30 min the IMF changed to northward IMF and remained steadily northward with a magnitude of 8 nT until hour 8. For northward IMF conditions reconnection occurred tailward of the cusp. In general the magnetospheric configurations were similar to those seen in previous MHD simulations for idealized IMF conditions [e.g., *Walker and Ogino*, 1989]. Particles were launched for a longer interval of time in the northward and dawnward IMF configurations than in the southward based on the assumption that during the first three hours of the simulation the magnetosphere had already responded to the southward IMF condition. Other solar wind parameters did not change with time. The solar wind density remained fixed at 10 cm^{-3}, and its velocity was -450 km/s in the x direction and the thermal pressure was 20×10^{-12} Pa. One feature of the simulation that was not included in many idealized simulations was a constant magnetic dipole tilt angle of 33°. The resulting hemispheric asymmetry was increased further because of the presence of an IMF B_x. Besides tilting the dayside magnetosphere the tilt and the B_x depressed the plasma sheet below $z = 0$ and warped it downward in the center versus the flanks.

[9] The entry of the high energy particles into the magnetosphere is strongly affected by the presence of open magnetic field lines. The variation of the fraction of open magnetic flux on the inner boundary as a function of time (Figure 2) reflects the morphological evolution of the model magnetosphere. For southward IMF the fraction of open flux is more than half. After the transition to dawnward IMF the fraction of open flux decreased for about 45 min and then stabilized and increased slightly. After the transition to northward IMF the fraction of open magnetic flux decreased

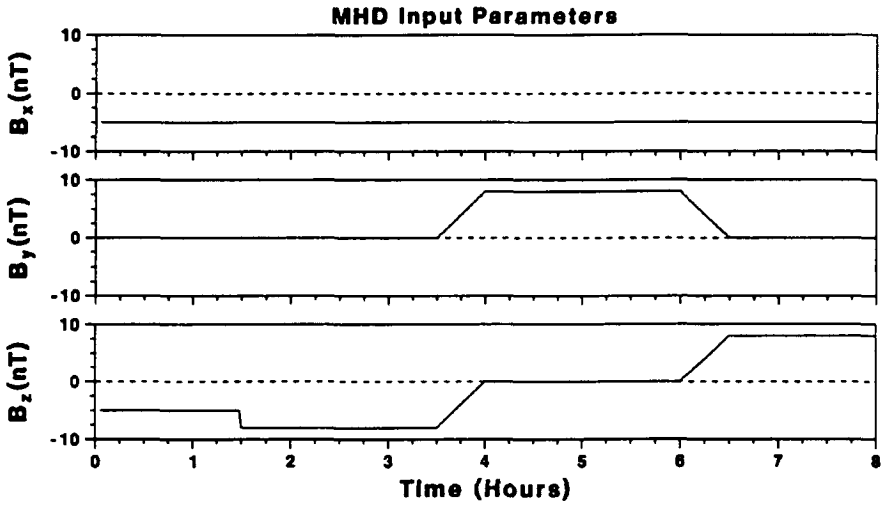

Figure 1. MHD input parameters. This figure shows the IMF conditions used to drive the MHD simulation as a function of time.

to an even lower level. Overall we arranged the simulation's driving conditions to be appropriate for generating a series of representative magnetospheric states. Launching a constant upstream flux in this system allowed us to attribute changes in the particle population in the magnetosphere to the effect of the magnetospheric configuration.

[10] The particle trajectories were calculated in the time varying fields from the MHD simulation and they experi-

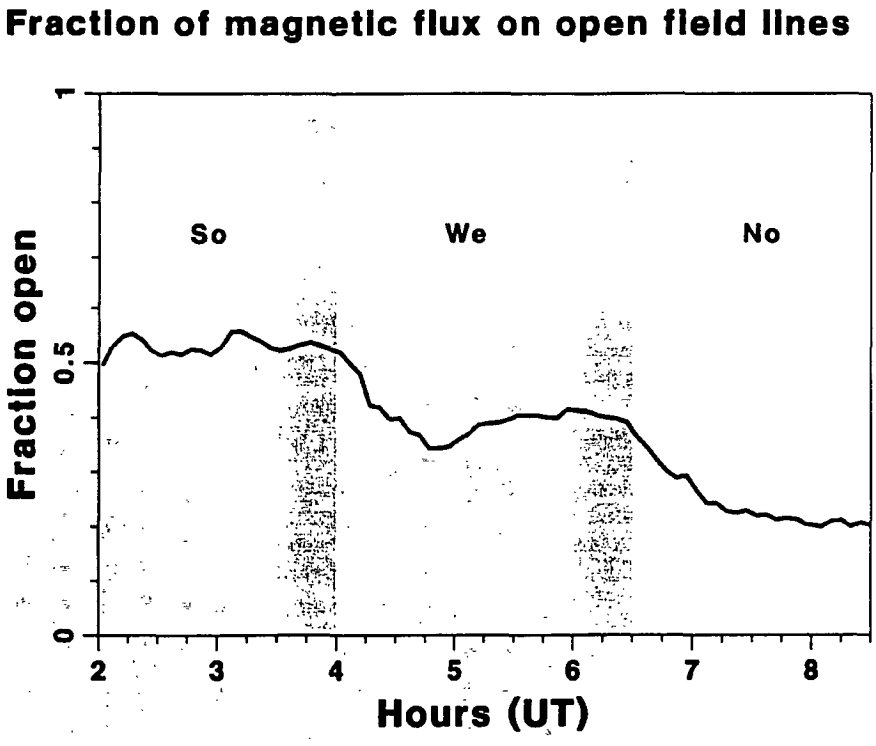

Figure 2. Fraction of open magnetic flux as a function of time. This was calculated by integrating the amount of open and closed flux through the inner boundary sphere at 4.5 R_E and dividing the amount of open flux by the total. The shaded bands indicate the times when the IMF was changing. The IMF direction is also indicated: "So" stands for southward, "We" for dawnward and "No" for northward.

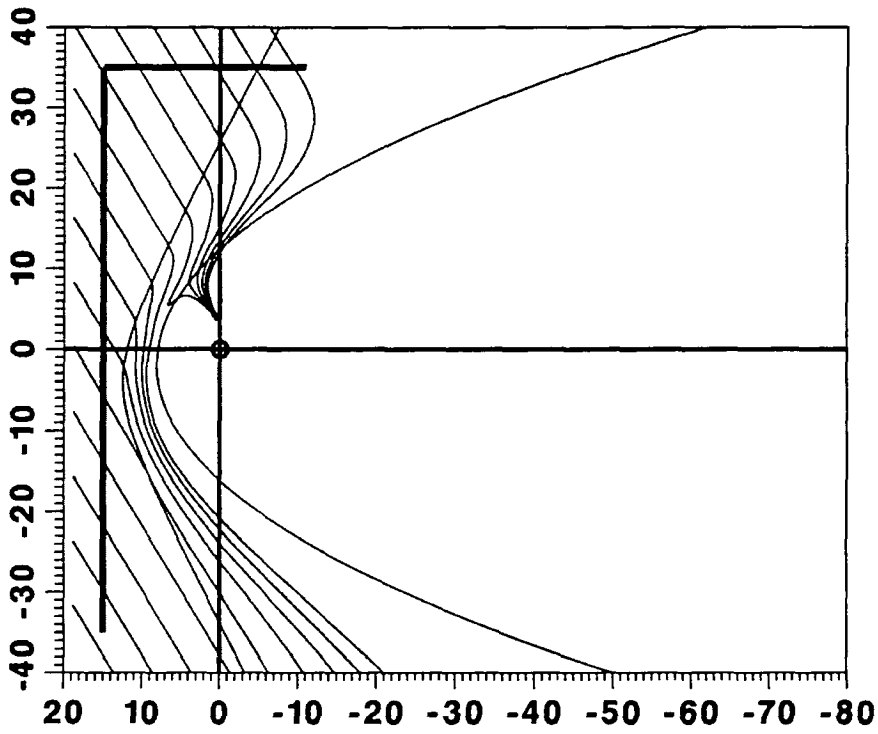

Figure 3. Particle launches for southward IMF. In this figure all items are at or projected into the $y = 0$ plane. The thin lines are magnetic field lines begun at $y = 0$ at the sunward boundary. Particles were launched on planes whose locations are indicated by the heavy lines. The other curves are fits to the magnetopause and bow shock and the $x = 0$ and $y = 0$ planes. The small circle represents the location of the Earth. Note the presence of dipole tilt and B_x.

enced different field configurations as time advanced. This was done by interpolating linearly in time between snapshots of the simulation fields taken every four minutes. Protons were launched every minute between simulation hours 3.0 to 8.0, while ^{3}He ions were launched only for southward IMF, i.e. between hours 3 and 3.5. A total of 9.4 million protons were launched, as well as about 1 million ^{3}He ions. High energy particles from the Sun reach the Earth streaming along interplanetary magnetic field lines [*Flückiger*, 1990]. We therefore launched our test particles (protons and ^{3}He ions) upstream of the magnetosphere in the solar wind. Figure 3 shows where they were launched for southward IMF. Particles were launched near the sunward boundary on a plane in the solar wind at $x = 15$ R_E extending between -35 and 35 R_E in y and in z. SEP particles from a single distant source arriving at the Earth along interplanetary field lines will arrive either parallel to or anti-parallel to the interplanetary field lines. Because the IMF B_x was negative particles that enter the system from the sunward direction were moving along magnetic field lines. Particles that are moving along field lines should enter the simulation system at other locations where field lines are directed into the system as well. All locations at the side, bottom or top boundary where field lines were directed into the simulation region were presumed to be particle sources. For example, for the southward IMF case particles were launched along the top boundary as well as the front boundary as well as at x = 15 R_E (Figure 3). Because particle distributions were modified by interaction with the bow shock we wanted to confine our launches to upstream of the bow shock. We therefore launched only in the region $x > -11$ R_E near where the bow shock intersects the system boundary; with this limit, however, some particles were launched in the magnetosheath because the bow shock position varied in time and this limit was an approximation.

[11] The particles were distributed in velocity space as a kappa distribution [*Christon et al.*, 1988] with a κ coefficient of 0.5. The formula for a kappa distribution function is $F(E) \sim (1 + E/\kappa E_T)^{-\kappa-1}$ where E is the energy and E_T is the thermal energy. For $E \gg E_T$ this becomes a power law with a coefficient of $-(\kappa + 1)$. The thermal energy used was set to a value near 40 keV. The energy range of particles launched was between 0.1 and 50 MeV. Particles below 100 keV were not included in the distribution because our study concerned particles above typical magnetospheric energies; and particles above 50 MeV have Larmor radii comparable to the system size also were not included. The launched distribution was isotropic except for the fact that only particles with velocities into the simulation system were included.

[12] Particles reaching the outer boundaries of a box with edges at $x = 18$, $x = -100$, y = ±40 and z = ±40 were removed as were those reaching a 4.5 R_E radius sphere centered on the Earth which is outside the simulation inner

boundary at 3.5 R_E. The particles reaching this boundary were considered to have precipitated. Particle 'hits' were collected at planar and spherical virtual detectors [*Ashour-Abdalla et al.*, 1993]. Particles that cross these surfaces have the time, positions and velocities of their crossing recorded. Particle fluxes and other quantities can be calculated from these values. Note that in the results shown in this paper flux at a virtual detector is the omnidirectional flux; i.e. the contributions of all the particles crossing a given virtual detector surface from any direction in a given region (chosen to be 1 R_E^2 squares) are added together. The flux at virtual detectors scale with the source in the upstream solar wind. Because we launched particles from $x > -11$ R_E only, we neglected particles that could arrive on open field lines that reached the simulation boundary tailward of the bow shock. Because the $\mathbf{E} \times \mathbf{B}$ drift in the solar wind was small compared to the velocities of the energetic particles, they usually did not convect to these parts of the polar cap either. This left part of the polar cap empty in our results. If our system size in y and z had been large enough to include all open field lines on the sunward side, the polar cap would probably have been more completely filled.

[13] Since we carried out our calculations using a time dependent IMF we must ask how our assumed time dependence (Figure 1) influences the results. In this idealized problem we want to show how particles enter the magnetosphere for a given IMF orientation. Therefore we want the magnetosphere to reach a quasi-steady configuration consistent with each IMF direction. However, trapped particles can remain in the model magnetosphere for a long time compared to the time between IMF orientations. Even after the IMF reaches a quasi-steady state for a given IMF some of the particles may have entered the magnetosphere when the IMF had a different orientation. To help us understand the effects of the time dependence on our results we carried out a series of calculations of particle trajectories for which the electric and magnetic fields were held constant. For these runs we used the electric and magnetic fields from single time steps in the MHD simulations. By comparing the time dependent results with the results from these snapshots we can estimate the significance of the time dependence.

3. Calculation Results

[14] At the beginning of the particle calculations, at hour 3.0, the IMF was in a southward orientation, and remained so until hour 3.5 at which time the IMF began its transition to a dawnward (positive B_y) orientation. Recall that there was a constant B_x throughout the entire simulation. At hour 4.0 the IMF transition was complete. During the southward IMF condition reconnection takes place on the dayside and in the magnetotail. Omnidirectional particle fluxes (protons / area · time) during the interval from hours 3.0 to 3.5 are shown in Figure 4. The upper panel shows the fluxes at the $z = 0$ plane and the lower panel shows the $y = 0$ plane for the interval between hours 3.0 and 3.5. Fits to the bow shock and magnetopause in the MHD simulation are shown as black curves. The dotted curves are the inner boundary of the particle calculation at 4.5 R_E. Nonzero fluxes appear just inside the inner boundary because the fluxes are collected in 1 R_E^2 domains. One important feature of the results at this and subsequent times was how effective the magnetospheric magnetic fields were in shielding the magnetosphere from the high energy solar protons. The bow shock and the magnetopause reflected most incoming protons. Note that the omnidirectional flux of particles upstream of the bow shock was often greater than the incident flux of particles launched. This was because of the contribution of particles reflected from the bow shock; recalling that particles passing through virtual detector planes in either direction were added to compute the omnidirectional flux, whereas in the incident flux all ions cross an upstream virtual detector in the same direction. There is a region of low omnidirectional flux, relative to adjacent magnetosheath and magnetospheric regions, just outside the magnetopause on the dawn side. This region contains open field lines that extend dawnward away from the Earth and then southward to the bottom boundary where particles were not launched during this interval. The ^{3}He ions we launched under southward IMF qualitatively followed the distribution of the protons but their flux within the magnetosphere was generally lower relative to their upstream abundance.

[15] A significant number of ions did penetrate the magnetosphere. We have observed two entry mechanisms for the ions we launched. As we will see later, ions with energies greater than about 10 MeV have Larmor radii large enough that they can directly penetrate the magnetosphere on the dayside, while lower energy ions moved along open field lines into the magnetosphere. The coefficient of adiabaticity κ, the square root of the ratio of the particle Larmor radius to the field line curvature [*Büchner and Zelenyi*, 1989] for these energetic particles often fell to values of around 1 or less and they can experience non-adiabatic behavior. This κ is not to be confused with the κ coefficient in the distribution function. In our simulation the directly penetrating particles were energetic enough to experience non-adiabatic behavior over large regions of the magnetosheath and magnetosphere. The locations of open field lines were of primary importance in determining particle entry for the majority of the particles, which were at energies below 1 MeV. Where the magnetic field was weak or had a small radius of curvature entry was enhanced.

[16] Note the effect of dipole tilt and B_x in Figure 4. Because of these factors the plasma sheet was warped such that it was lower (in z) near midnight than on the dusk or dawn flanks and parts of it fell below $z = 0$. In the magnetotail between hours 3.0 and 3.5 the protons were mainly confined to the plasma sheet while the lobes were nearly empty. Protons in this plasma sheet were confined within a band around 5 R_E high in z, but were spread out all along the plasma sheet in y, reflecting the thinness of the plasma sheet for southward IMF. During this time interval (hours 3.0 to 4.0) the protons entered mainly on the front side of the magnetosphere, often through the northern cusp region, visible in Figure 4 near $z = 6$, $x = 3$ R_E. The weak field and open field lines at the northern cusp allowed particles to access the inner magnetosphere. Once inside the magnetosphere, they sometimes became quasi-trapped and began drifting around the Earth. While a few protons remained trapped over a relatively long term (hours) most of them reached the inner boundary or entered the plasma sheet and

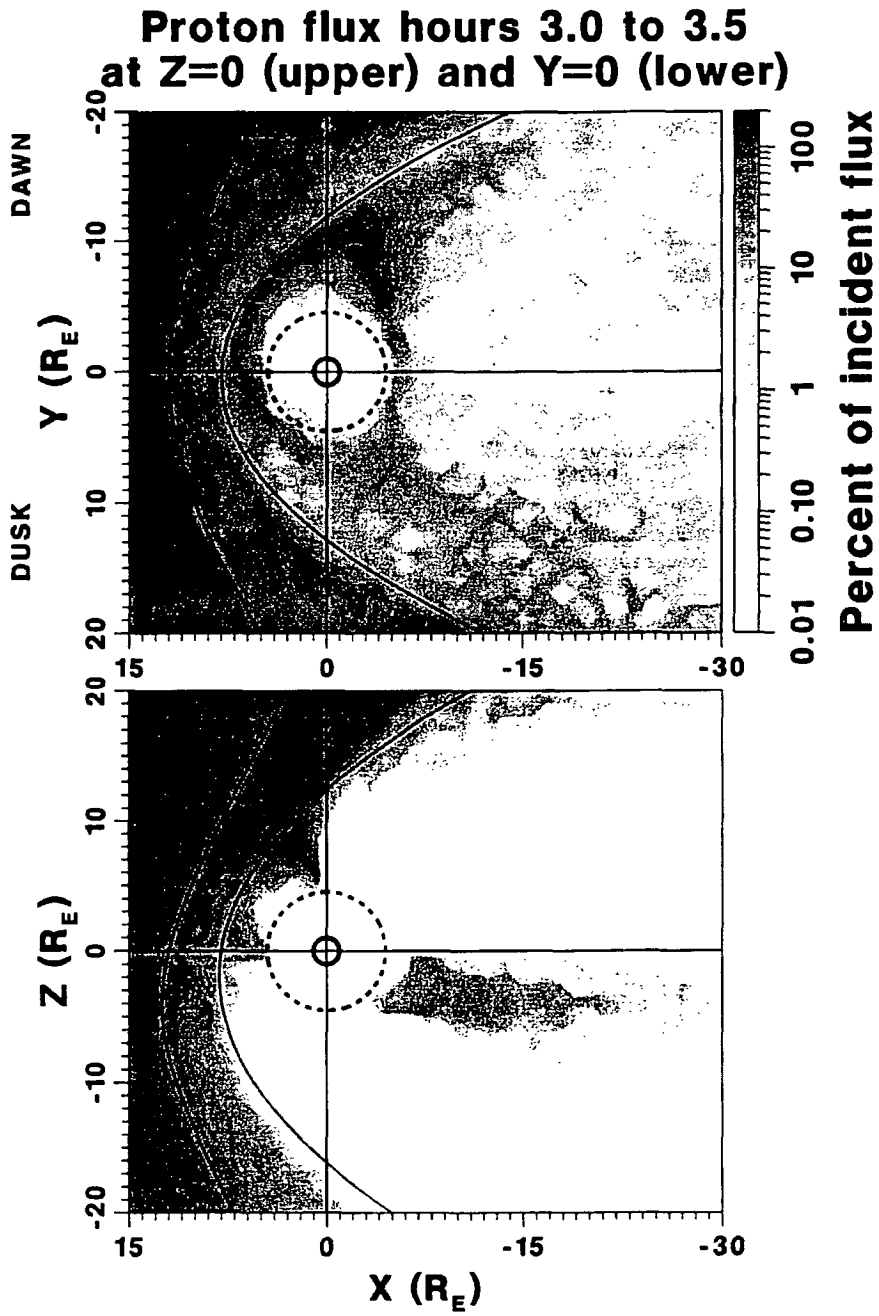

Figure 4. Omnidirectional particle fluxes accumulated at virtual detectors. The upper panel shows the fluxes at the $z = 0$ plane and the lower panel shows the $y = 0$ plane for the interval between hours 3.0 and 3.5. Fits to the bow shock and magnetopause in the MHD simulation are shown as black curves. The dotted curves are the inner boundary of the particle calculation at 4.5 R_E. Nonzero fluxes appear just inside the inner boundary because the fluxes are collected in 1 R_E^2 domains. In the magnetosphere, the regions of highest flux had the order of a thousand hits (one particle can hit a virtual detector more than once) per domain at a virtual detector while the smallest fluxes could reflect a single hit.

were subsequently lost tailward or at the flanks. The particles that became trapped for long enough to completely circle the Earth were adiabatic for the most part and could be energized by the changing local magnetic field responding to the IMF. The cusp, plasma sheet and the region of quasi-trapped particles are clearly visible in Figure 4, bearing in mind the effect of dipole tilt and consequent plasma sheet warping. The high omnidirectional flux of protons visible in the noon-

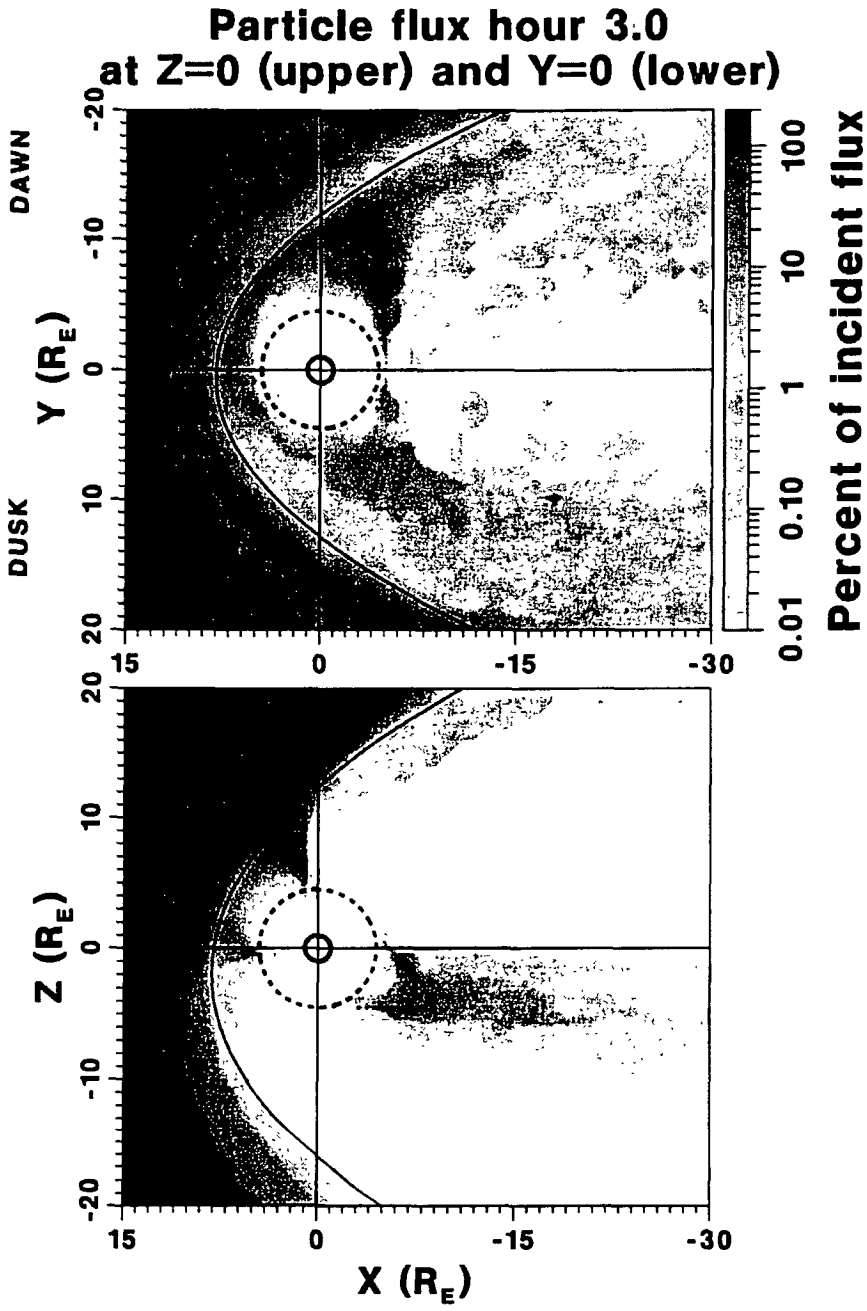

Figure 5. Omnidirectional particle fluxes accumulated at virtual detectors for a time independent case. This calculation used a snapshot of the MHD at 3.0 hours. The format is the same as for Figure 4.

midnight meridian just above $z = 0$ inside the magnetopause are quasi-trapped particles circulating around the Earth. Ions in the equatorial region would probably have approached the Earth more closely, and remain trapped longer, but were lost at the inner boundary at 4.5 R_E. It must be kept in mind that for most of these particles the trapping is temporary and they leave close field lines again later, frequently returning upstream. While the ions often bounced wildly through the magnetotail the overall motion was primarily dawn to dusk in the direction of the gradient drift in the tail and trapped particles circled the Earth in the expected clockwise sense. It can be seen that omnidirectional ion fluxes (Figure 4) reach levels comparable to their fluxes in the solar wind for the quasi-trapping region and the cusp.

[17] To help evaluate the role of time dependence we also ran particles in a snapshot of the fields from the MHD simulation taken at 3.0 hours. The flux pattern for this case is shown in Figure 5. Comparing this to Figure 4, it can be seen that the two patterns are remarkably similar. There seems to be a decrease in penetration into the magneto-

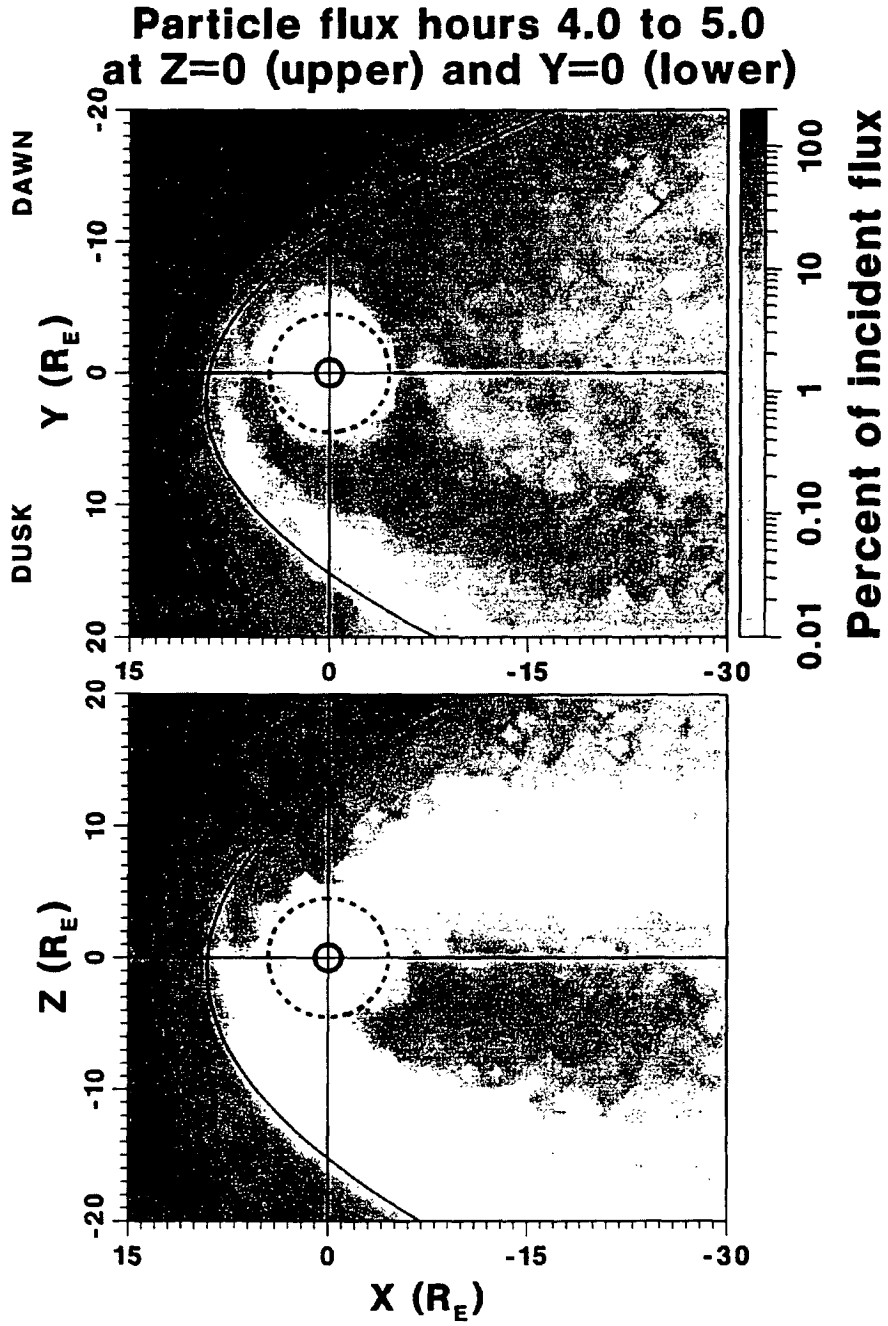

Figure 6. Particle fluxes between hours 4.0 and 5.0. The format is the same as for Figure 2. This interval had a steady dawnward IMF.

sphere in the time-independent case versus the time dependent case. This may mean that penetration is enhanced in the time dependent case, but the effect is evidently secondary in the case of a slowly varying magnetosphere.

[18] Between hours 4.0 and 6.0 the IMF was dawnward. For this configuration open field lines extended through the dawn flank. This defined the primary entry region for the protons. On the other hand there is a region with relatively few or no particles just inside the dusk side magnetopause in the equatorial plane beginning at about 7 R_E from the noon-midnight meridian and extending to the dusk side boundary (Figures 6 and 7). Once they entered the plasma sheet protons spread out toward the dusk side. Omnidirectional fluxes in the quasi-trapping region, the plasma sheet and the cusp decreased considerably during the interval between simulation hours 4.0 and 5.0 (Figure 6). The examination of single particle trajectories indicated that particles tended to

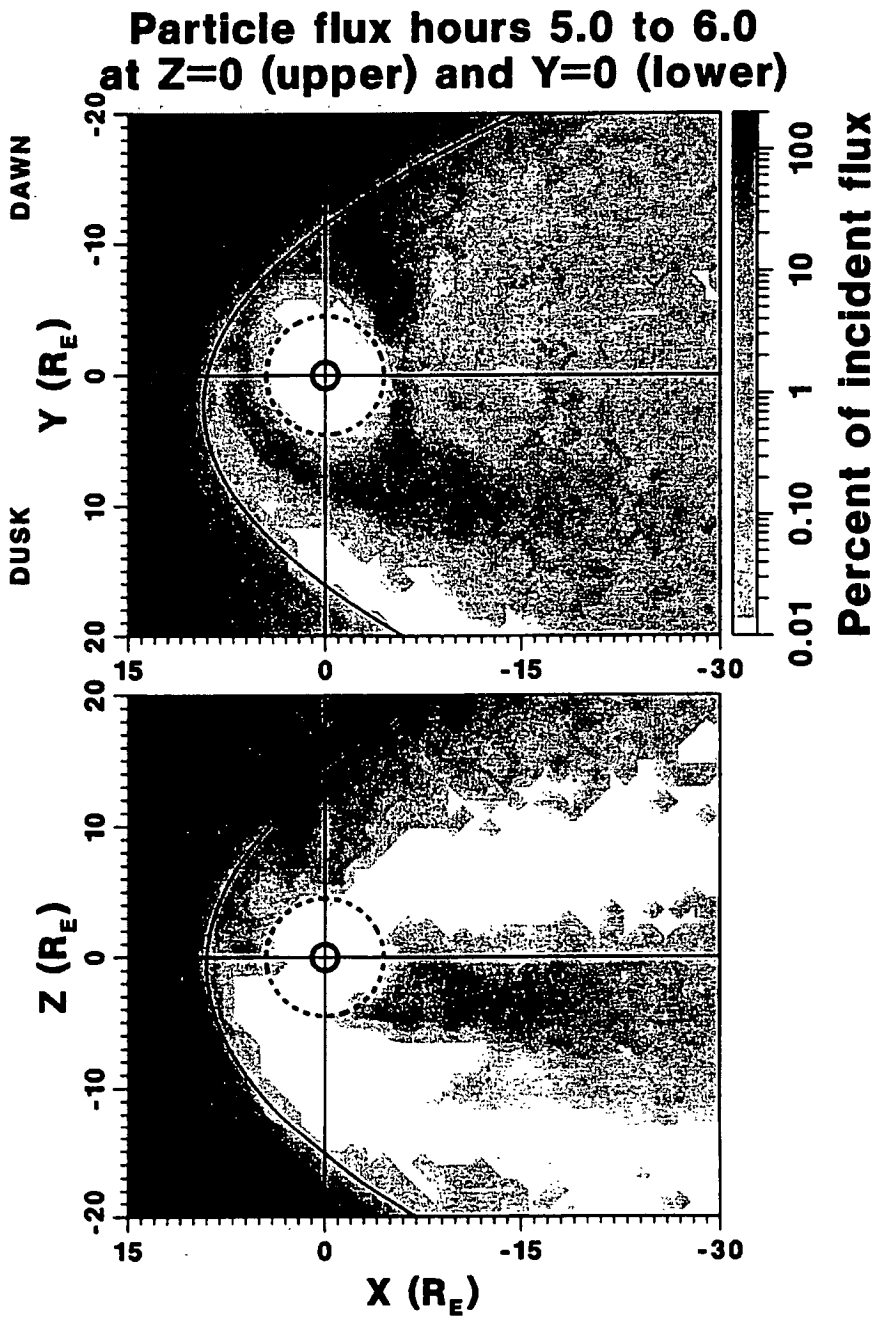

Figure 7. Particle fluxes between hours 5.0 and 6.0. The format is the same as for Figure 2. This interval had a steady dawnward IMF.

approach the near Earth region from the magnetotail or on the dayside due to direct penetration that was always present. As can be seen by comparing Figure 4 and Figure 6 there was a lower flux of trapped and quasi-trapped particles (between about 9 R_E and the inner boundary) during the dawnward IMF interval. For this configuration, protons can most easily access the magnetotail from the dawn side flank, but these protons most commonly exit down the tail and do not reach the inner magnetosphere. The location of maximum flux in the plasma sheet (comparing Figures 4 and 6) is now further from the Earth, as well as less intense. Because the field lines in the magnetotail are no longer as highly stretched protons bounce further from the equatorial plane.

[19] The interval between 5.0 and 6.0 had a flux distribution qualitatively similar to that of the previous hour (Figures 6 and 7). The main difference is an overall decrease in flux and a concentration of high flux to a localized region

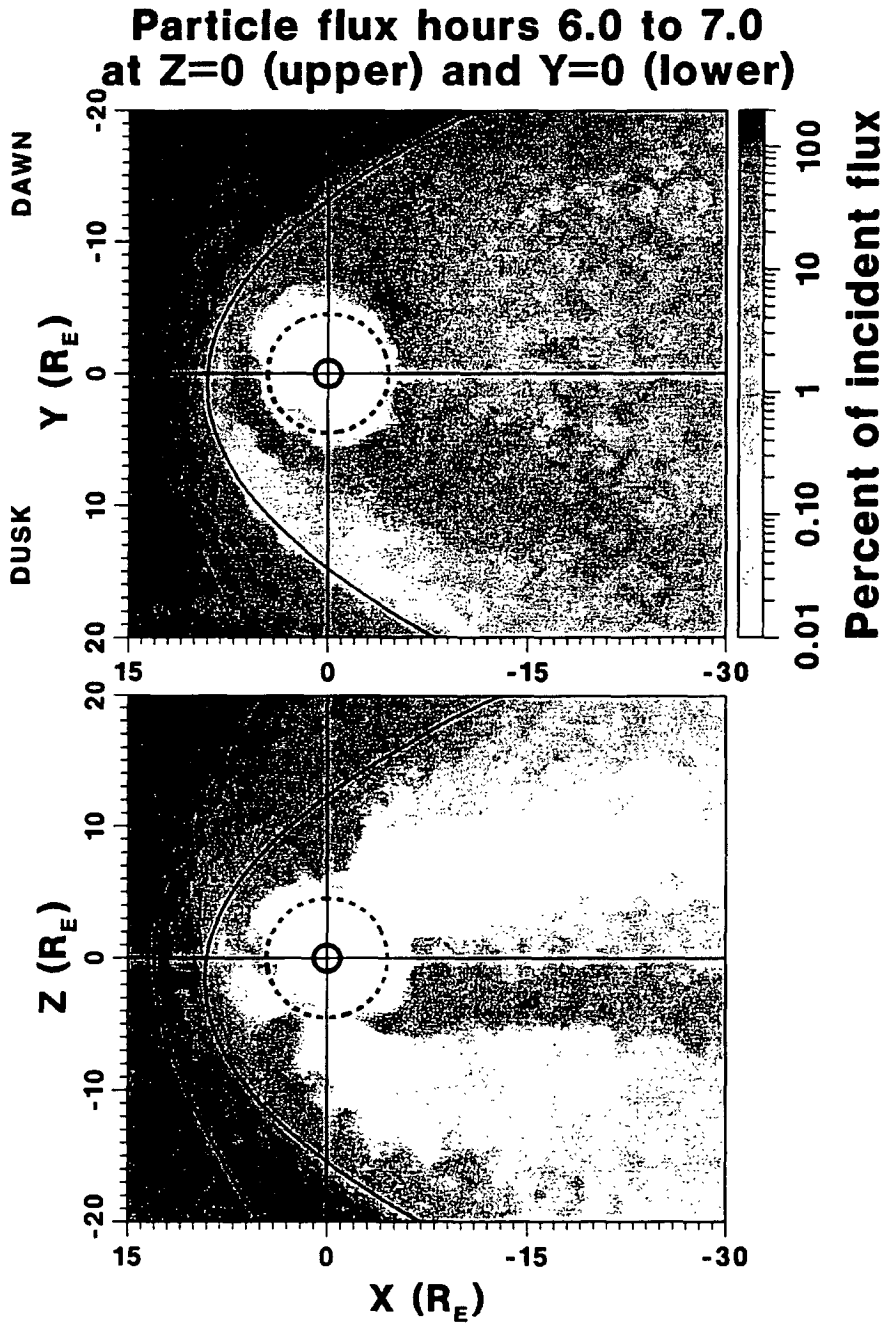

Figure 8. Particle fluxes between hours 6.0 and 7.0. The format is the same as for Figure 2. The first half an hour of this interval was during the transition from dawnward to northward IMF and the second half hour was for steady northward IMF.

on the dawn side that did not seem to correspond to any strong localized entry in the MHD simulation. Examining single particle trajectories indicates that transport in the magnetotail remained primarily from dawn to dusk. For the dawnward case the time independent simulation (not shown) gave results similar to the time dependent case. As was seen in the southward IMF case, however, magnetospheric fluxes in the time independent case seemed to be reduced slightly overall compared to the time dependent case. For both southward and dawnward IMF particles often partially orbit the Earth while mirror bouncing and then exit the magnetosphere, usually tailward or back into the magnetosheath. Others precipitate at the inner boundary after being trapped for a while. If the inner boundary had been closer to the Earth, these particles would presumably have remained trapped for a longer period.

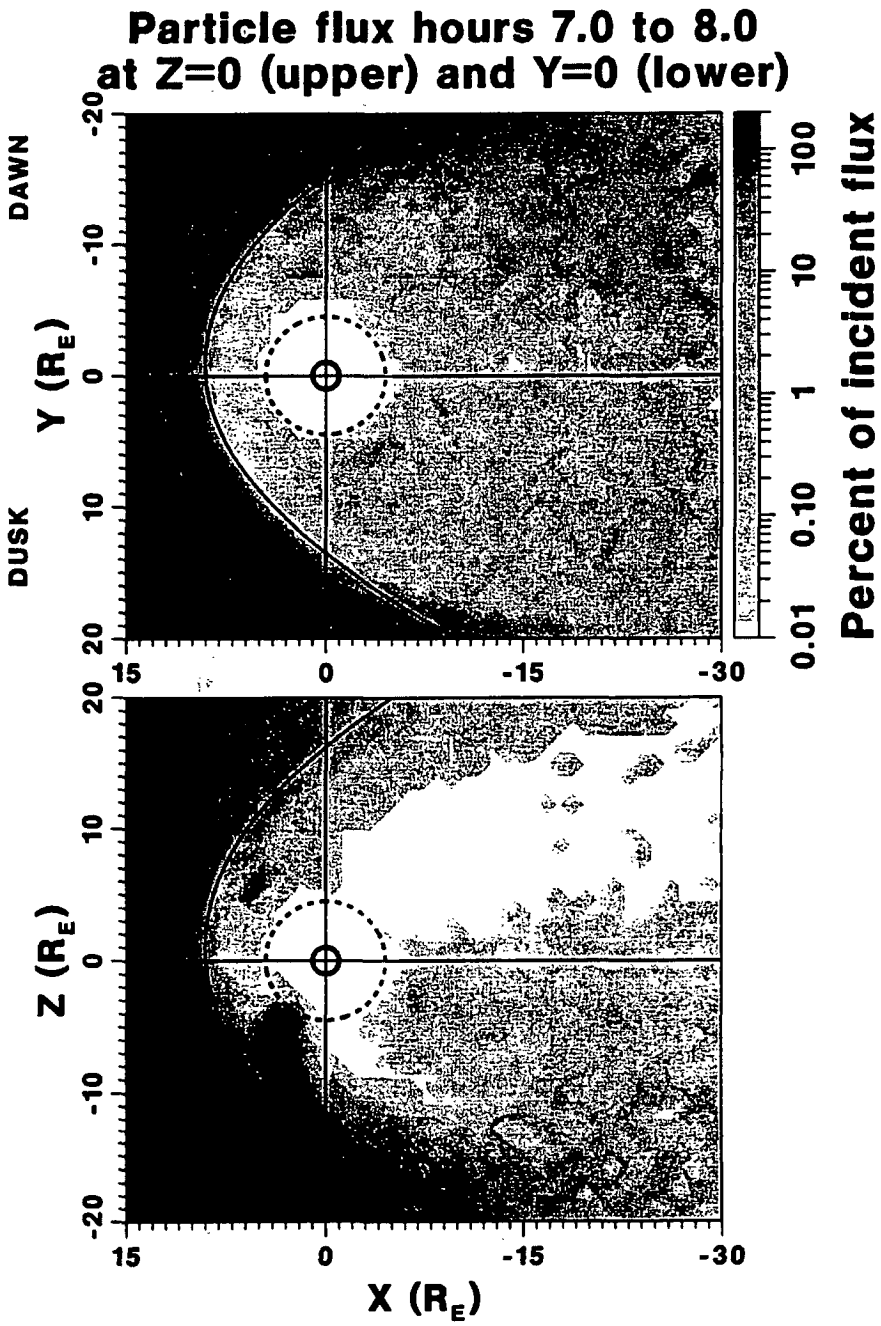

Figure 9. Particle fluxes between hours 7.0 and 8.0. The format is the same as for Figure 2. This interval had a steady northward IMF.

[20] From hour 6.0 to 6.5 the IMF changed from dawnward to northward, and then remained steady until hour 8.0. The asymmetry due to dipole tilt and IMF B_x caused more intense magnetic reconnection to take place in the Southern Hemisphere, tailward of the cusp, and therefore most open field lines extended southward. The examination of single particle trajectories indicated that the great majority of the ions in the northern hemisphere entered from a southward direction. Particle entry on the dawn side decreased and fluxes in the southern cusp increased as the field changed (Figure 8). The plasma sheet flux decreased although the maximum moved close to the Earth. The lobes on the dawn side contained a low level of energetic particle flux. This flux extends to the noon-midnight meridian plane below the plasma sheet.

[21] The flux from hour 7.0 to 8.0 decreased overall. The most dramatic feature is the high flux in the southern cusp (Figure 9). The magnetopause can be seen to be a strong

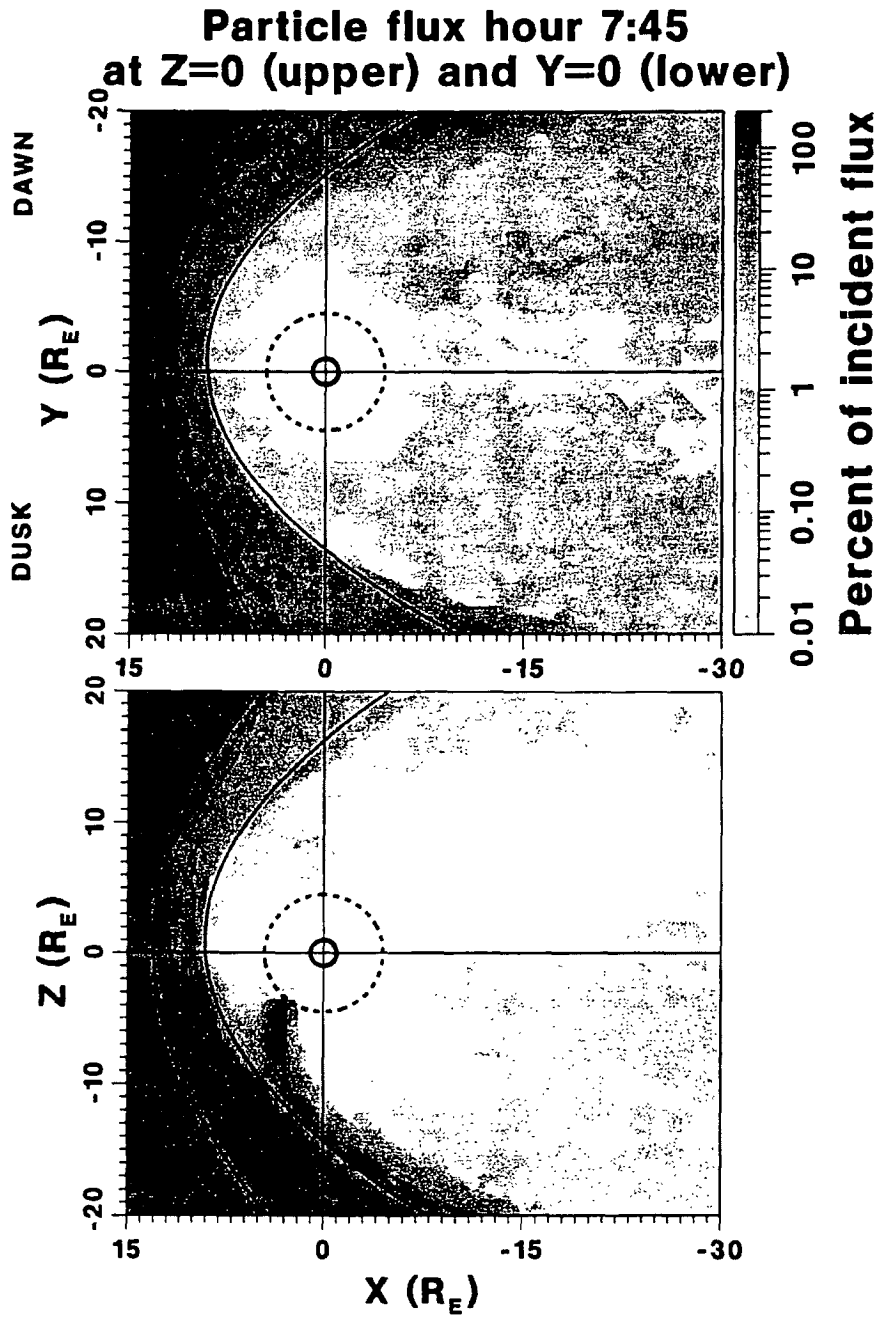

Figure 10. Omnidirectional particle fluxes accumulated at virtual detectors for a time independent case. This calculation used a snapshot from the MHD simulation at 7 hours 45 min. The format is the same as for Figure 9.

barrier to particle entry at this time. Particles enter through the southern cusp and high fluxes also occur on the dawn side LLBL region, though in this case particle drifts across the field and access to open field lines replaced convection on newly opened field lines [*Richard et al.*, 1994] as the main entry processes. When we ran a time independent case using a snapshot of the northward IMF magnetosphere, at 7 hours 45 min, we obtained an interesting result. While the results in the outer magnetosphere were comparable between the time dependent and time independent cases, there is much less flux in the inner magnetosphere in the vicinity of the equatorial plane in the time independent case (Figure 10). To understand this difference we examined the particles that occupied the inner magnetosphere in the time-dependent case. We found that these were trapped or quasi-trapped particles that had entered the inner magnetosphere

during earlier times when the IMF orientation was dawnward or southward. We conclude that there were no trapped or quasi-trapped particles observed during the quasi-steady northward IMF simulation that were launched while the IMF was northward.

[22] Although the ions were usually non-adiabatic and could gain or loose energy due to magnetospheric electric fields, the high energies of the launched particles relative to the electric potential across the magnetosphere caused energization within the magnetosphere to be of minor importance overall. The exceptions were particles gradient drifting around the Earth for a prolonged interval. These particles experienced adiabatic heating as the magnetic field changed. Waves in the inner magnetosphere that might heat ions further did not play a role in this calculation; even though there are expected to be MHD wave modes present in the simulation, because the sampling of the MHD simulation results every four minutes filtered out almost all waves. To understand the basic physics of particle entry it is instructive to examine the trajectories of single particles in the model system. The particle trajectories to be discussed now are protons that all precipitated onto the inner boundary. Particles of this type were chosen because transport into the near Earth region is important for our results. For southward IMF protons could access the inner magnetosphere near the northern cusp. One such proton (Figure 11) was launched at simulation time 3 hours and 32 min and had an initial energy of 107 keV and a 25° pitch angle. This particle began on a solar wind field line on the dawn side and moved toward the magnetosphere. At the magnetopause it experienced a brief interval with $\kappa < 1$ as it crossed from solar wind to closed field lines. After travelling tailward on the dawn side near the equatorial plane it was eventually scattered into a nearly perpendicular pitch angle. As it migrated toward the Earth and became trapped, which occurred near midnight, κ fell below 1.5. It became trapped and remained so for a prolonged period, finally precipitating after simulation hour 10. This particle experienced adiabatic heating while trapped and its final energy was 190 keV. While this particle was on open field lines only very briefly, it was the strongly curved field lines resulting from dayside reconnection that led to a decrease of κ allowing the particle to enter.

[23] A 611 keV proton launched at 6 hours 14 min simulation time, during the transition to northward IMF, is shown in Figure 12. As can be seen from its path in the solar wind the particle's motion is mainly field aligned there with a pitch angle of 27°. This particle began on solar wind field lines on the dawn side and reached the magnetopause where it became trapped in the magnetopause current layer with a mainly perpendicular pitch angle. It experienced $\kappa < 2$ only during one interval, which is on curved field lines in the magnetosheath. While in the magnetopause current layer it reached open field lines that it followed inward, and its pitch angle changed to greater than 160°. Later it gained more parallel velocity and precipitated. In Figure 13 we have plotted the trajectory of a proton of 390 keV launched at 6 hours 26 min simulation time with an initial pitch angle of 63°. As one would expect from the IMF direction at this time it approached the magnetosphere from the southern, dawnward direction. It crossed into the magnetosphere on the flanks of the magnetotail. Its large Larmor radius in the solar wind is apparent, and this allows it to cross directly from the solar wind to open field lines and finally to closed field lines. It moves on closed field lines to the inner boundary. Finally a definitely directly penetrating proton is shown that had an initial energy of 45 MeV and an initial pitch angle of 85° (Figure 14). It was launched at simulation time 6 hours and 45 min. It had a huge Larmor radius in the solar wind that tightened as it crossed the bow shock and magnetopause. This particle moved easily between different field line types until it struck the inner boundary. It experienced $\kappa < 2$ throughout much of its time in the magnetosphere.

[24] One way to demonstrate the magnetospheric configuration's control of the entry of high energy particles is to plot the population of the inner magnetosphere and the precipitation rate (Figure 15) as a function of time. The numbers in this figure were computed assuming that the upstream flux represents a total flux above 100 keV of 2.5×10^8 protons / $m^2 \cdot s$. This number is based on the differential flux for a typical SEP event at 100 keV taken from *Gloeckler* [1984]. The precipitation rate, i.e. precipitation onto the inner boundary at 4.5 R_E, shows a fairly systematic variation with IMF. Recall that the IMF was southward at first, then dawnward, and finally northward. Also keep in mind that part of the flux in the polar cap on open field lines that do not connect to the dayside has been omitted. During southward IMF the precipitation rate was relatively high, reflecting an abundance of open field lines and efficient transport into the inner magnetosphere. The rate decreased during the dawnward IMF interval and finally falls to a very low level during steady northward IMF. The trend is consistent with the decrease of open field lines that occurred as the IMF changed from northward to southward as shown in Figure 2.

[25] The number of protons at less than 7 R_E (Figure 15) can be taken to reflect the population of the inner magnetosphere in the model. While some of these protons were quasi-trapped in the inner magnetosphere, most of them remained only briefly in the inner magnetosphere before reaching the inner boundary or exiting the system, usually tailward or duskward. Only about 1% of the test protons remained in the inner magnetosphere for more than 15 min. Some protons were observed to make a nearly complete circle around the Earth then exit back into the magnetosheath. The initial increase of the population during southward IMF was evidently due to the system filling with protons as the calculation proceeded; particles could take a few minutes to reach this region. During southward IMF most protons entered the inner magnetosphere on the dayside. After the IMF turned dawnward the number entering the inner magnetosphere on the dayside decreased and highest concentration of arrival points (into the inner magnetosphere) was found dawnward of midnight. Evidently these were particles that entered the magnetotail on the dawnside open field lines and reached the inner magnetosphere. The overall population in the inner magnetosphere decreased during dawnward IMF as the region of particle arrival moved tailward. As the IMF changed to northward, the entry rate into the inner magnetosphere increased again, with protons arriving primarily from the dawn side. During this transition the number of particles in the inner magnetosphere increased, but this is due to the particles in the

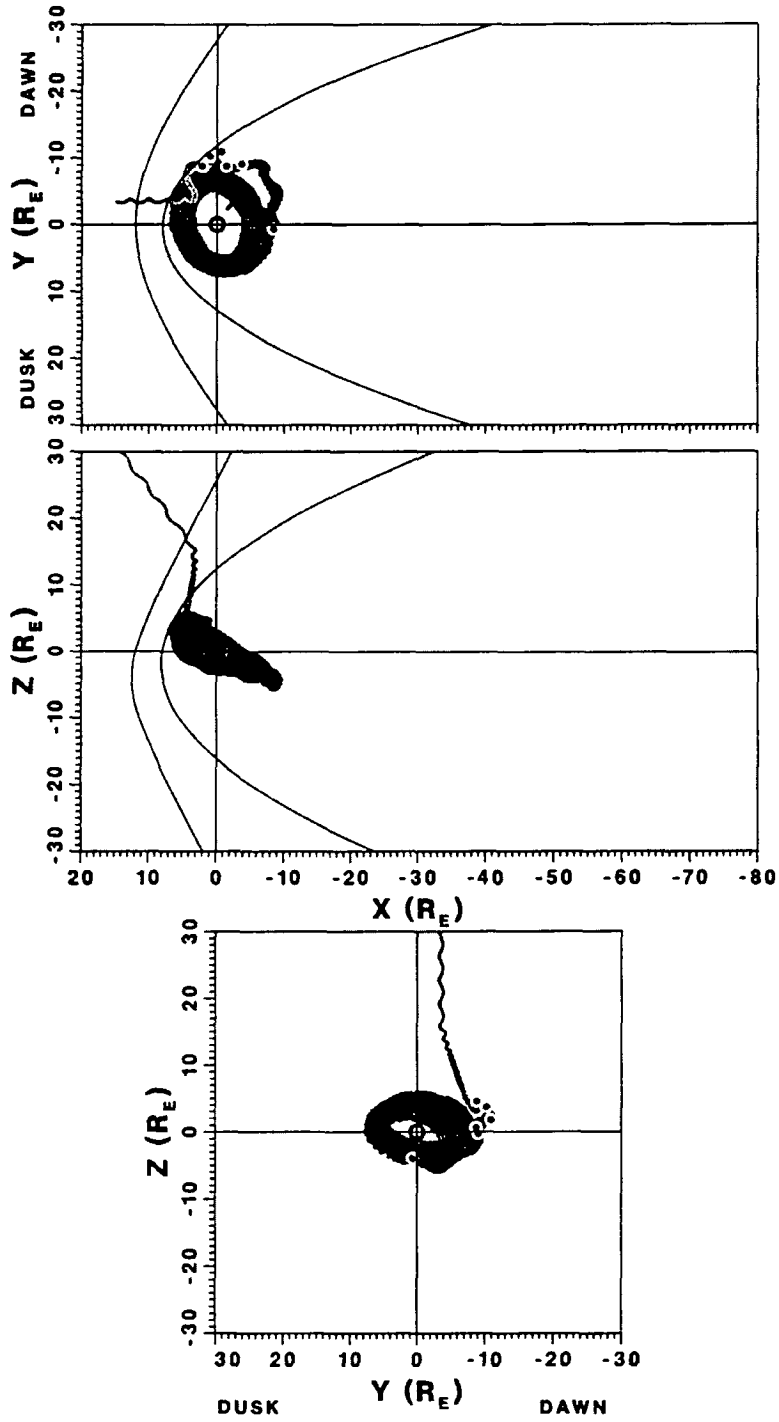

Figure 11. Proton trajectory shaded gray according to field line type. Shown are points along a particle trajectory projected onto the $z = 0$ (top panel), $y = 0$ (middle panel) and $x = 0$ (bottom panel) planes. Points where the particle was on closed field lines are dark gray and ones on solar wind field lines are medium gray. Because the total number of points had to be decimated to make this plot, the small number of points on open field lines are not shown. Filled circles along the trajectory in the top and bottom panels indicate the locations of local minimums of κ where $\kappa < 2$. In the middle panel, these points are behind the dense points where the particle is trapped and therefore are not shown. To limit the cluttering of the figure a filled circle was only plotted if it was at least 1.6 R_E away from the others.

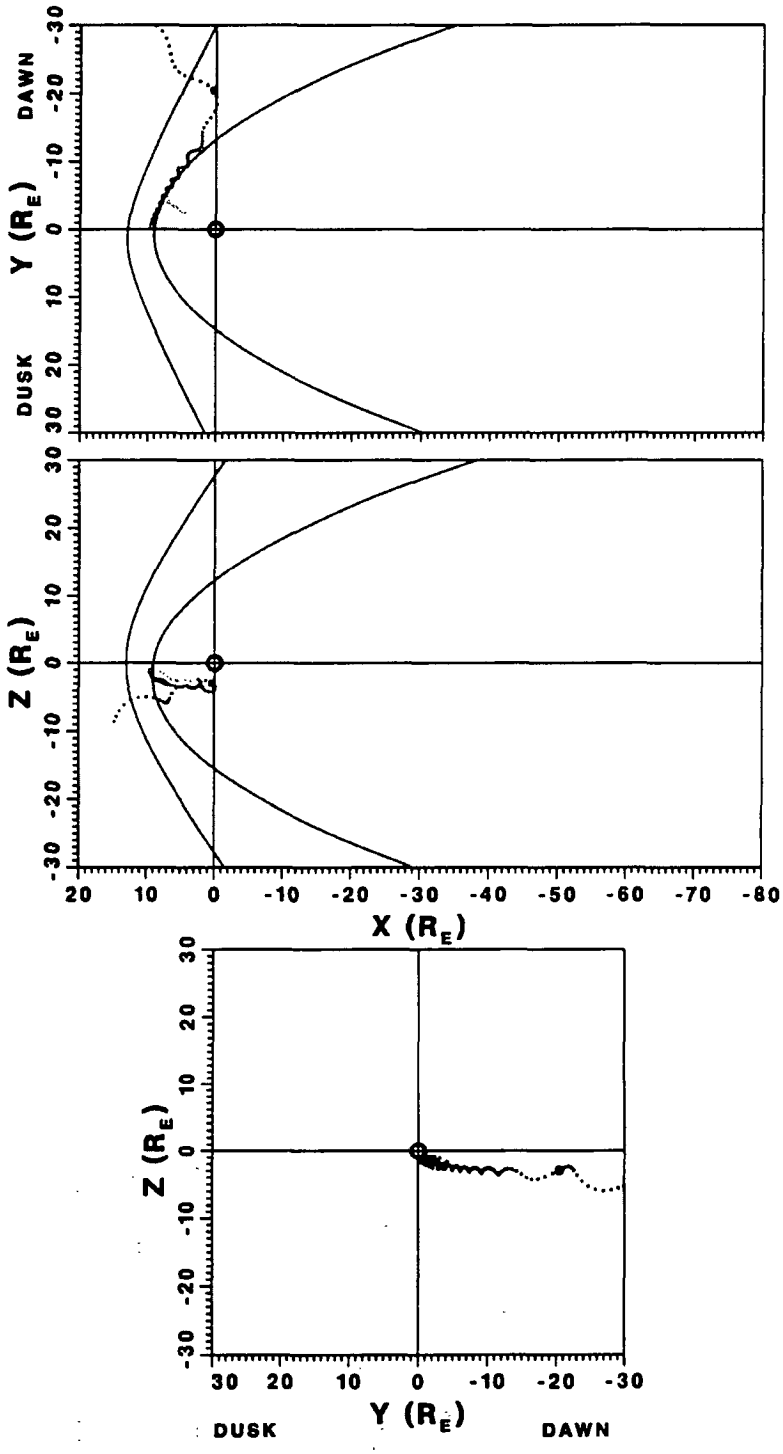

Figure 12. Proton trajectory shaded gray according to field line type. Shown are points along a particle trajectory projected onto the $z = 0$ (top panel), $y = 0$ (middle panel) and $x = 0$ (bottom panel) planes. Points where the particle was on open field lines are light gray and ones on solar wind field lines are medium gray. Filled circles indicate points that were local minimums of κ where $\kappa < 2$ and were more than 1.6 R_E apart.

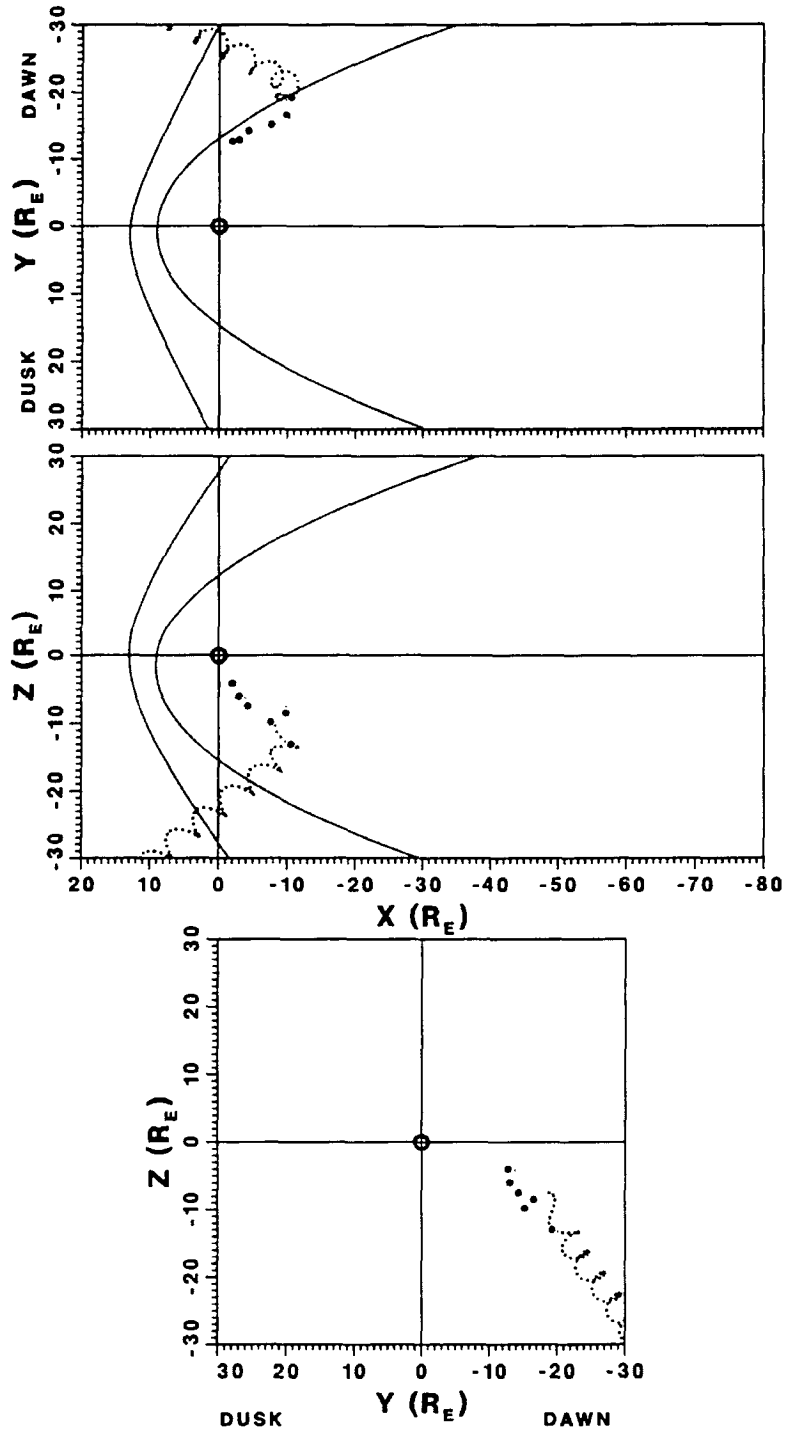

Figure 13. Proton trajectory shaded gray according to field line type. Shown are points along a particle trajectory projected onto the $z = 0$ (top panel), $y = 0$ (middle panel) and $x = 0$ (bottom panel) planes. Points where the particle was on open field lines are light gray and ones on solar wind field lines are medium gray. Filled circles indicate points that were local minimums of κ where $\kappa < 2$ that were more than 1.6 R_E apart.

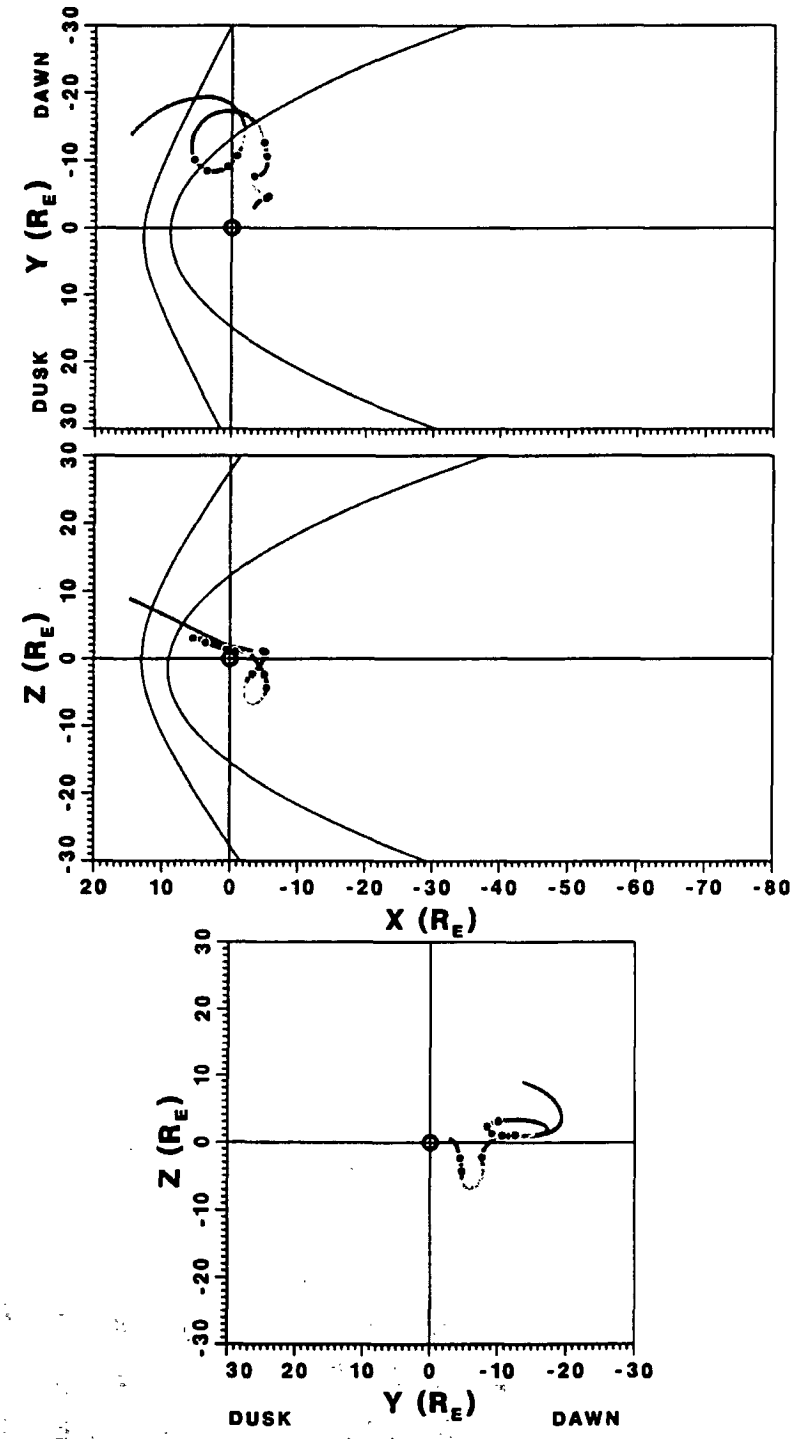

Figure 14. Proton trajectory shaded gray according to field line type. Shown are points along a particle trajectory projected onto the $z = 0$ (top panel), $y = 0$ (middle panel) and $x = 0$ (bottom panel) planes. Points where the particle was on open field lines are light gray, ones on closed field lines are dark gray and ones on solar wind field lines are medium gray. Filled circles indicate local minimums of κ where $\kappa < 2$ that were more than 1.6 R_E apart.

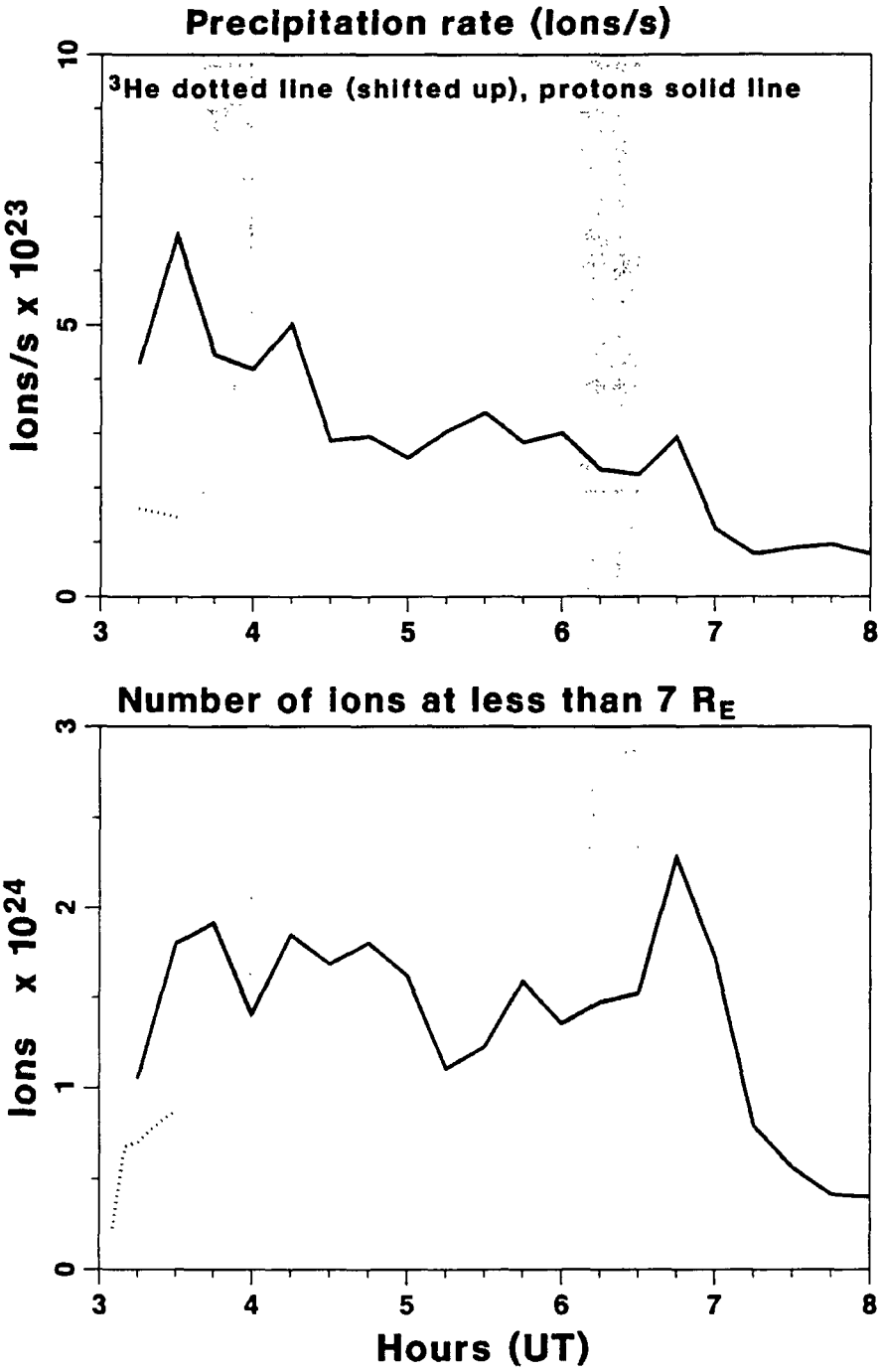

Figure 15. Precipitation rate and population of the inner magnetosphere as a function of time. The gray bands indicate the times when the IMF was changing. The top panel shows the precipitation rate onto the inner boundary of the simulation for an upstream flux of 2.5×10^8 protons / $m^2 \cdot$ sec. Data points are 15 min apart. The bottom panel shows the number of particles between 7 R_E and the inner boundary for the same upstream flux, with data points every five minutes.

southern cusp, not trapped or quasi-trapped particles. As steady northward IMF conditions continued few particles reached the inner magnetosphere with most of these briefly entering near the southern cusp.

[26] The ^{3}He ion abundance is enhanced during impulsive SEP events. We calculated ^{3}He ion trajectories for southward IMF only. The flux distribution for these particles was qualitatively similar to that of the protons that are

shown in Figure 4, but the fluxes within the magnetosphere were reduced relative to the upstream flux. For the purpose of comparison with protons we plotted the population of the inner magnetosphere and precipitation for these particles in Figure 15 as if they had the same upstream flux as the protons. It can be seen that they entered the inner magnetosphere and precipitated at a lower rate (relative to their upstream flux) than the protons. This is consistent with the role of κ in particle entry. For particles of the same energy the velocity of a proton will be greater than that of an ^{3}He ion by a factor of the square root of the mass ratio. The mass of an ^{3}He ion is three times the mass of a proton while the charge doubles. This leads to a proton having a Larmor radius 15% larger than an ^{3}He ion of the same energy.

4. Conclusions

[27] We have seen that in our calculation high energy particles' access to the magnetosphere was strongly controlled by the IMF. For a steady proton source the omnidirectional proton fluxes in some locations in the magnetotail varied by a factor of 100 as the IMF changed. Transport into the inner magnetosphere varied by a factor of 5. A southward IMF condition allowed the greatest access to the magnetosphere of the IMF conditions studied, dawnward IMF less, and northward IMF considerably less. The cusp was an important entry region for the high energy particles for northward and southward IMF, while the dawn side flank was the dominant entry location for dawnward IMF. *Fritz et al.* [1999] reported that energetic particles are frequently observed in the cusp region. While they have ruled out an SEP source for events seen on August 27, 1996 it is possible that some of these events are related to SEPs. Relative to their initial high energy, the SEPs in our calculations usually did not gain or lose much energy. The exceptions were particles that remained trapped long enough to gain or lose energy adiabatically during IMF transitions. It was likely that because of our inner boundary at 4.5 R_E some particles that otherwise would remain trapped and possibly further energized are lost. We can easily estimate this energization. In being transported from 6 R_E to 4 R_E at midnight an equatorial pitch angle particle conserving μ would increase in energy by a factor of 2.8. The transport of SEPs in our calculation often involved nonadiabatic motion. Particles usually entered the magnetosphere while they were not adiabatic. Non adiabatic motion could also be important for the transport of particles onto trapped or quasi-trapped paths.

[28] Time-independent calculations gave results that were quite similar to the time dependent ones in the outer magnetosphere, even though the latter were obtained by accumulating data through half an hour to an hour while the magnetosphere was slowly varying. This indicates that for a slowly varying magnetosphere a time independent calculation is adequate for modeling energetic particle entry. This can be attributed to the fact that high energy particles rapidly precipitated, became trapped or exited the magnetosphere. There were hints that particle penetration was enhanced in the time dependent case, suggesting that a rapidly varying magnetosphere could experience significantly enhanced particle penetration. On the other hand, trapped particles experienced the consequences of IMF changes. These particles, however, remained a minor part of the total population in the inner magnetosphere during southward and dawnward IMF. The trapped particles were affected by IMF changes largely through adiabatic changes that affected the particle orbits by a relatively small amount and changed their energies. During northward IMF, when particles from the solar wind did not become trapped, the trapped particle population consisted solely of particles that had entered the magnetosphere during earlier IMF orientations. The population of trapped particles was reduced in our calculation, however, by the removal of particles at 4.5 R_E from the Earth.

[29] Because IMF conditions typically undergo much more rapid variations than in this idealized case particle entry into the magnetosphere may be even more complex than in our results. In this calculation the residence time of the vast majority particles in the magnetosphere was much less than the duration of transitions in the IMF (half an hour). For rapid variations in the IMF, especially when a shock strikes the magnetosphere, the entry process would probably be modified. We argued in the introduction that if the SEP proton flux in the solar wind during an intense gradual proton event could easily enter the magnetosphere it would dominate the plasma sheet population in the energy range above 0.1 MeV. Our model indicates that the SEP flux within the magnetosphere does become comparable to the solar wind flux in parts of the magnetosphere depending on IMF orientation. The near Earth magnetotail under southward IMF is one instance of this.

[30] **Acknowledgments.** The authors would like to thank L Zelenyi for helping define the problem and V Peroomian, D Schriver and G Reeves for helpful discussions This work was supported by NSF grant ATM 98-19879 and NASA ISTP grant NAG5-6689 Computing resources were provided by the National Resource Allocations Committee (NRAC), the San Diego Supercomputer Center and the Office of Academic Computing at UCLA.

[31] Arthur Richmond thanks Joan Feynman and another reviewer for their assistance in evaluating manuscript 2001JA000099

References

Ashour-Abdalla, M , J Berchem, J Büchner, and L M Zelenyi, Shaping of the magnetotail from the mantle Global and local structuring, *J Geophys. Res.*, *98*, 5651, 1993.

Ashour-Abdalla, M., et al., Ion sources and acceleration mechanisms inferred from local distribution functions, *Geophys Res Lett* , *24*, 955, 1997

Baker, D. N , T I. Pulkkinen, X Li, S G Kanekal, J B Blake, R S Selesnick, M. G Henderson, G D. Reeves, H E. Spence, and G Rostoker, Coronal mass ejections, magnetic clouds, and relativistic magnetospheric electron events: ISTP, *J Geophys Res* , *103*, 17,297, 1998.

Blanc, M., et al., Source and loss processes in the inner magnetosphere, *Space Sci. Rev*, *88*, 137, 1999

Büchner, J., and L. M. Zelenyi, Regular and chaotic charged particle motion in magnetotail-like field reversals, I, basic theory of trapped motion, *J Geophys. Res* , *94*, 11,821, 1989

Christon, S. P., D G. Mitchell, D. J. Williams, L. A Frank, C. Y Huang, and T E. Eastman, Energy spectra of plasma sheet ions and electrons from ~50 eV/e to ~1 MeV during plasma temperature transitions, *J. Geophys Res.*, *93*, 2562, 1988.

Fennell, J. F , Access of solar protons to the Earth's polar caps, *J Geophys Res* , *78*, 1036, 1973.

Flückiger, E. O., Solar Cosmic Rays, *Nucl Phys. B*, *22B*, 1, 1990

Frank, L. A , et al , Observation of plasmas and magnetic field in Earth's distant magnetotail. Comparison with a global MHD model, *J Geophys Res* , *100*, 19,177, 1995

Fritz, T. A., J. Chen, R. B Sheldon, H E. Spence, J F. Fennell, S Livi, C. T. Russell, and J. S. Pickett, Cusp energetic particle events measured by Polar spacecraft, *Phys Chem Earth C*, *24*, 135, 1999.

Hudson, M. K., S. R. Elkington, J. G. Lyon, V. A. Marchenko, I. Roth, M. Temerin, and M. S. Gussenhoven, *Radiation Belts: Models and Standards, Geophys. Monogr. Ser.*, vol. 97, edited by J. F. Lemaire et al., p. 57, AGU, Washington, D.C., 1996.

Gloeckler, G., Characteristics of solar and heliospheric ion perturbations near Earth, *Adv. Space Res.*, *4*(2–3), 127, 1984.

Gussenhoven, M. S., E. G. Mullen, and D. H. Brautigam, Phillips Laboratory space physics division radiation models, *Radiation Belts: Models and Standards, Geophys. Monogr. Ser.*, vol. 97, edited by J. F. Lemaire et al., p. 93, AGU, Washington, D.C., 1996.

Kallenrode, M.-B., Space Physics, Springer-Verlag, New York, 1998.

Lin, R. P., Solar particle acceleration and propagation, *Rev. Geophys.*, *25*, 676, 1987.

Ogino, T., R. J. Walker, M. Ashour-Abdalla, A global magnetohydrodynamic simulation of steady magnetospheric convection, in *Proceedings of the Second International Conference on Substorms (ICS-2)*, edited by J. R. Kan, J. D. Craven and S.-I. Akasofu, 545 pp., Geophys. Inst. Univ. of Alaska, Fairbanks, 1994.

Raeder, J., R. J. Walker, and M. Ashour-Abdalla, The structure of the distant magnetotail during long periods of northward IMF, *Geophys. Res. Lett.*, *22*, 249, 1995.

Reames, D. V., Particle acceleration at the Sun and in the heliosphere, *Space Sci. Rev.*, *90*, 413, 1999.

Reames, D. V., L. M. Barbier, T. T. Von Rosenvinge, G. M. Mason, J. E. Mazur, and J. R. Dwyer, Energy spectra of ions accelerated in impulsive and gradual solar events, *Astrophys. J.*, *483*, 515, 1997.

Richard, R. L., R. J. Walker, and M. Ashour-Abdalla, The population of the low latitude boundary layer by solar wind ions when the interplanetary field is northward, *Geophys. Res. Lett.*, *21*, 2455, 1994.

Richard, R. L., R. J. Walker, T. Ogino, and M. Ashour-Abdalla, Flux ropes in the magnetotail: Consequences for ion populations, *Adv. Space Res.*, *20*(4/5), 1017, 1997.

Rodriguez-Pacheco, J., J Sequeiros, L. Del Peral, E. Bronchalo, and C. Cid, Diffusive-shock-accelerated interplanetary ions at several energies during the solar cycle 21 maximum, *Solar Phys.*, *181*, 185, 1998.

Shea, M. A., and D. F. Smart, History of solar proton observations, *Nuclear Phys. B*, *39A*, 16, 1995.

Walker, R. J., and T. Ogino, Global magnetohydrodynamic simulations of the magnetosphere, *IEEE Trans. Plasma Sci.*, *17*, 135, 1989.

Walker, R. J., R. L. Richard, T. Ogino, and M. Ashour-Abdalla, The response of the magnetotail to changes in the IMF orientation: The magnetotail's long memory, *Phys. Chem. Earth*, *24/1–3*, 221, 1999.

M. Ashour-Abdalla, Department of Physics and Astronomy, University of California at Los Angeles, Los Angeles, California 90095, USA.

M. El-Alaoui and R. L. Richard, Institute of Geophysics and Planetary Physics, University of California at Los Angeles, Los Angeles, California 90095, USA. (rrichard@igpp.ucla.edu)

R. J. Walker, Department of Earth and Space Science, University of California at Los Angeles, Los Angeles, California 90095, USA.